

The role of the K-channel and the active-site tyrosine in the catalytic mechanism of cytochrome *c* oxidase

Vivek Sharma^{a,b,*} and Mårten Wikström^{c,*}

^a Department of Physics, Tampere University of Technology, FI-33101, Tampere, Finland.

^b Department of Physics, University of Helsinki, Helsinki, Finland.

^c Institute of Biotechnology, University of Helsinki, FI-00014, Helsinki, Finland.

Corresponding authors;

Vivek Sharma, vivek.sharma@tut.fi

Mårten Wikström, marten.wikstrom@helsinki.fi

Keywords: electron transfer, proton pumping, neutral tyrosyl radical

Abbreviations: molecular dynamics, MD; density functional theory, DFT; cytochrome *c* oxidase, CcO.

FOOTNOTE: All amino acid numbering corresponds to the cytochrome *c* oxidase from *Bos taurus*.

Abstract

The active site of cytochrome *c* oxidase (*CcO*) comprises an oxygen-binding heme, a nearby copper ion (Cu_B), and a tyrosine residue that is covalently linked to one of the histidine ligands of Cu_B . Two proton-conducting pathways are observed in *CcO*, namely the D- and the K-channels, which are used to transfer protons either to the active site of oxygen reduction (substrate protons) or for pumping. Proton transfer through the D-channel is very fast, and its role in efficient transfer of both substrate and pumped protons is well established. However, it has not been fully clear why a separate K-channel is required, apparently for the supply of substrate protons only. In this work, we have analysed the available experimental and computational data, based on which we provide new perspectives on the role of the K-channel. Our analysis suggests that proton transfer in the K-channel may be gated by the protonation state of the active site tyrosine (Tyr244), and that the neutral radical form of this residue has a more general role in the *CcO* mechanism than thought previously.

1. Introduction

Complex IV, or cytochrome *c* oxidase (CcO), reduces molecular oxygen (O₂) to water, and couples the free energy released to proton translocation across the inner membrane of mitochondria and bacteria [1-5]. The proton pumping activity creates a proton electrochemical gradient across the membrane, which is used to drive the synthesis of ATP. Since its discovery as a true proton pump [6], cytochrome *c* oxidase (CcO) has been at the center-stage of bioenergetics research. Based on a large amount of experimental work, various aspects of enzyme function have been elucidated [1-5]. For instance, crystallographic studies provided an atomic view of the interior of the enzyme, and helped the identification of electron and proton transfer paths [7-11] (Fig. 1). Spectroscopic studies have advanced our knowledge on the structure of the active site intermediates that form during catalysis [12-17]. Furthermore, time-resolved electrometric experiments provided the first clues into how charge translocation events are linked to the catalytic reactions [16,17]. Overall, our current understanding of the molecular mechanism of O₂ reduction is fairly complete, and can be described as shown in Fig. 2.

The electron-proton coupling in CcO is a non-trivial issue because for every electron transferred to the active site, a substrate proton is consumed at the same site, and an additional proton is pumped across the membrane [6]. Various models explaining the coupling between electrons and protons have been proposed, and indeed basic principles of redox-coupled proton pumping are well understood [1-5]. However, details of some of the elementary reactions still need to be sorted out [3].

One such remaining problem is the precise role of the K-channel. This proton transfer pathway is named after Lys319 (Fig. 1), which is conserved in all A-type oxidases [18]. It connects the N-side of the membrane via Lys319 to the crucial tyrosine (Tyr244) at the active site (Fig. 1). The latter residue is covalently linked to one of the histidine ligand of Cu_B (His240), and is responsible for the transfer of an electron and a proton to the active site during early stages of the reaction. However, recent quantum-chemical studies have indicated a much wider role of Tyr244 in the function of CcO [19,20], as will be discussed below.

It is well-known that in the early stages of the reaction cycle ($\mathbf{P}_M \rightarrow \mathbf{F}/\mathbf{F}_H \rightarrow \mathbf{O}/\mathbf{O}_H$), the K-channel is not used. It is also generally accepted that the transfer of the substrate proton in the $\mathbf{O}/\mathbf{O}_H \rightarrow \mathbf{E}/\mathbf{E}_H$ step [21-23], and also possibly in the $\mathbf{E}/\mathbf{E}_H \rightarrow \mathbf{R}$ transition [17], occurs via the K-channel. The question then arises why the “substrate protons” required for chemistry are not taken from the K-channel in the oxidative half of the catalytic cycle as well. Is there a thermodynamic bias in favour of the D-channel, or is there a kinetic barrier associated with the proton transfer in the K-channel? Here,

we combine available experimental and computational data with additional calculations and analysis, and discuss mechanistic aspects of the K-channel and the active site tyrosine.

2. The K-channel and the role of active site tyrosine in the oxidative phase

The \mathbf{P}_M' (\mathbf{P}_M with reduced heme *a*) \rightarrow \mathbf{F} transition of the oxidative phase can be considered to comprise an electron transfer from heme *a* to TyrO^{*} forming TyrO⁻ in \mathbf{P}_R [4,19]. It is well-known from FTIR experiments that Tyr is deprotonated in states \mathbf{P}_R and \mathbf{F} [24,25]. This means that in the transition $\mathbf{P}_R \rightarrow \mathbf{F}$, which is coupled to uptake of a net proton from the N-side of the membrane, the substrate proton must have gone to the ligands of Fe or Cu_B (O²⁻ or OH⁻, respectively). Since the oxygenous ligand of Cu_B (OH⁻) is directly hydrogen bonded to the nearest water molecule of the water wire from Glu242, as found in molecular dynamics simulations [26,27], a rapid proton transfer from the D-channel to the ligand of Cu_B can be expected, forming state \mathbf{F} [26,27] (Figs. 2 and 3).

Our molecular dynamics (MD) simulation data on the \mathbf{P}_R state [27] shows that the ligands of the binuclear center (BNC) may also connect to the N-side of the membrane, via Lys319, which in its protonated form [28] rapidly adopts an “UP” conformation (Fig. 3). Hence, proton transfer from the N-side to the BNC, through the K-channel, could be as kinetically efficient as from the D-channel. This raises the important question of what prevents the proton transfer from the K-channel in the $\mathbf{P}_R \rightarrow \mathbf{F}$ transition. One key point to note here is that in order to supply the substrate proton to the Cu_B ligand via the K-channel, the proton would have to pass via TyrO⁻. We propose that it is the low proton affinity ($pK_a < 7$) of TyrO⁻, as shown by FTIR data [25], that kinetically prevents the protonation of the BNC from the K-channel. This FTIR data showing that the tyrosine is unprotonated throughout the oxidative phase of the catalytic cycle [25] stands in contrast to earlier density functional theory (DFT) and continuum electrostatic calculations, which suggested that Tyr is protonated [29-31]. However, more recent DFT calculations agree with the FTIR data [20]. Whilst both FTIR and DFT data thus show that Tyr has a low pK_a during the oxidative phase of the catalytic cycle, quantum mechanical (QM) calculations on small models representing a Cu_B system suggest that the oxygenous ligand of the latter has a higher proton affinity than the tyrosinate (by ca. 2 kcal/mol or ~ 1.5 pK units) [32]. In fact, Blomberg [20] recently found in QM calculations on a much larger BNC model that an \mathbf{F} state with tyrosine protonated lies at a ~ 7.5 kcal/mol higher energy level than the state where the OH⁻ ligand of Cu_B is protonated instead.

In summary, the chemical proton in the $\mathbf{P}_R \rightarrow \mathbf{F}$ transition is taken up by the OH^- ligand of Cu_B rather than by the tyrosinate for thermodynamic reasons. However, the reason this proton is not taken via the K-channel is kinetic: the barrier for the necessary transient protonation of the tyrosinate before the proton reaches the Cu_B ligand on the other side of the BNC is likely to be too high due to the low $\text{p}K_a$ of the tyrosine.

2.1. The \mathbf{F} state

The substrate proton taken up into the unstable \mathbf{P}_R state yields state \mathbf{F} , and we have already discussed why this proton is taken up via the D-channel into the OH^- -ligand of Cu_B , forming water. This water molecule may now remain as a weakly bound Cu_B ligand (state \mathbf{F}), or may dissociate away (state \mathbf{F}_H) (see Fig. 2). In the latter case, the Cu_B center attains a trigonal geometry [19]. We found the free energy difference between the two states to be only 2-3 kcal/mol (\mathbf{F}_H higher in energy). Interestingly, in both states, but especially in \mathbf{F}_H , a considerable fraction of the unprotonated tyrosine attains a free radical nature (Fig. 2, see also ref. 19), which means that the major part of the electron is on the copper ($\text{Cu}_B[\text{I}]$) [19]. Hence, one reason for the high redox potential of the \mathbf{F} states is the neutral tyrosine radical [19], which therefore has functional importance beyond the \mathbf{P}_M state, its original unique location (Fig. 2). Blomberg [20] has recently reached a similar conclusion based on independent QM calculations.

2.2. The $\mathbf{F}/\mathbf{F}_H \rightarrow \mathbf{O}_H$ transition

The next transition in the catalytic cycle is $\mathbf{F}/\mathbf{F}_H \rightarrow \mathbf{O}_H$. In this relatively slower transition (~ 1 millisecond), a state analogous to \mathbf{P}_R , called \mathbf{F}_R here, is not observed experimentally, which is either due to a higher energy of the latter state, or to its formation being slower than its conversion [33]. However, our earlier DFT calculations shed some light on the possible structure of this intermediate, and showed that upon formation of \mathbf{F}_R , part of the added electron distributes on Tyr, and part on the heme/ Cu_B system [19]. This causes a local protonic shift yielding the active-site structure $\text{Fe}[\text{III}]\text{-OH}^- \text{Cu}[\text{II}]\text{-OH}^- \text{TyrO}^-$ [19] (Fig. 2). Note that the Cu_B center attains a structure similar to that in \mathbf{P}_R ($\text{Fe}[\text{IV}]=\text{O}^{2-} \text{Cu}[\text{II}]\text{-OH}^- \text{TyrO}^-$), as well as the same overall charge. Therefore, the $\text{p}K_a$ of TyrO^- is again likely to stay low and effectively prevent the protonation of the BNC from the K-channel (see above), so that the protonation of the BNC occurs from the D-channel through Glu242 and intervening water molecules [27].

2.3. States $\mathbf{O_H}$ and \mathbf{O}

We have recently proposed the structure of the fully-oxidised activated state $\mathbf{O_H}$ [19] that forms primarily upon completion of the oxidative phase ($\mathbf{P_M} \rightarrow \mathbf{F} \rightarrow \mathbf{O_H}$) (Fig. 2). In $\mathbf{O_H}$, the cross-linked tyrosine once again retains a radical character, and Cu_B is weakly ligated by the hydroxy ligand of heme a_3 in a strained fashion [19]. It is this structural arrangement that apparently provides part of the driving force required for proton pumping upon arrival of the next electron, which does not occur upon electron transfer to the “relaxed” \mathbf{O} state [19,21]. Blomberg and Siegbahn have recently proposed a very similar structure for the $\mathbf{O_H}$ state [34]. Our computationally proposed structure of the relaxed \mathbf{O} state is one in which the ferric heme iron is ligated by a water molecule, which in turn is strongly hydrogen bonded to the OH^- ligand of Cu_B , and Tyr remains as tyrosinate [19] (Fig. 2, but see below in this section). Blomberg and Siegbahn [35], on the other hand, have proposed that the “relaxed” \mathbf{O} state is formed from $\mathbf{O_H}$ by uptake of an additional proton into the BNC from the N-side. This state, labeled $\mathbf{O_P}^+$, has a neutral protonated tyrosine, Cu(II) and Fe(III) are ca. 3.8 Å apart, and share a bridging hydroxyl ligand [35, *cf.* 36]. Interestingly, the FTIR data by Gorbikova et al. [25] suggested that the tyrosine would be partially protonated in state \mathbf{O} , with a $\text{p}K_a$ of 6.6. Such a protonation of the BNC need not require net proton uptake from the medium, but could be due to local proton transfer from Lys319 [25].

3. Opening of the K-channel in the reductive phase

It has been suggested that during catalytic turnover the Cu_B center has an elevated redox potential in the $\mathbf{O_H}$ state (at least 100 mV higher than the other redox centers) [22], which is most likely due to the strained structure of the BNC, and radical character of Tyr [19] (see section 2.3). The recent DFT calculations by Blomberg [20] also suggest a high redox potential for the $\mathbf{O_H}$ state. Our DFT calculations show that upon formation of one-electron reduced state ($\mathbf{O_{H,R}}$), the electron preferably goes to the TyrO^* [19], yielding a formal structure in which Cu_B is cuprous and tyrosine is anionic ($\text{Cu}_B[\text{I}]-\text{TyrO}^-$), in agreement with experimental data [22,25]. What is interesting to note is that this situation is not encountered in any of the earlier reactions ($\mathbf{P_M} \rightarrow \mathbf{F} \rightarrow \mathbf{O_H}$) (Fig. 2). Therefore, we suggest that a sharp rise in the $\text{p}K_a$ of TyrO^- is expected to occur only in this state [see also 32], leading to protonation of the tyrosinate from the N-side, in agreement with the FTIR data [25]. The $\mathbf{E/E_H} \rightarrow \mathbf{R}$ step is least studied experimentally, mainly due to technical issues [16,17]. However, DFT calculations have been performed on some of the states of this transition, which suggest that the tyrosine may partially attain a neutral radical state together with high-spin ferrous heme (Fe[II]) ligated by a water

molecule in the E_H state [20]. However, as alluded to above, FTIR data show that tyrosine is most likely protonated in this state [25], which leads to an alternative structure of the BNC; Fe[III]-OH-Cu[I] TyrOH. Here, the two metals may be bridged by the hydroxo ligand of Fe, in a relatively strained fashion.

We suggest that proton transfer via the K-channel is effectively gated by the protonation state of Tyr244. A substrate proton is supplied through the K-channel only in the transitions of the reductive phase when Cu_B is cuprous, and the pK_a of Tyr244 exceeds 7. The protonated side chain of Tyr most likely dissociates from the hydroxy group of the farnesyl chain of high-spin heme, thereby, allowing proton transfer to the oxygenous ligands of the BNC, a notion also supported by the X-ray structure [36].

4. Is Lys319 the gating element in the K-channel?

In multiple independent MD simulations of the P_R state [27], we observed that the side chain of protonated Lys319 undergoes a conformational change, and moves closer to Tyr (and also to the BNC) by ca. 5 Å, in agreement with earlier simulation results [37-41]. In recent work, Woelke et al. [41] also observed a similar up-flip of the Lys319 side chain in the P_R state, but provided a different reasoning for the non-functionality of the K-channel. They suggested that in the $P_M \rightarrow F$ transition, a P_R -like state is not stabilized. Instead, a transient state forms in which the electron temporarily resides on heme a_3 , and not on the Cu_B center (on Tyr as in P_R). This means that in their case Tyr retains the neutral tyrosyl radical character, and heme iron has the structure $Fe[III]=O^{2-}$. They suggested that this results in a lower pK_a of Lys319. Due to the neutral nature of Lys319, a proton transfer to the BNC via this pathway does not take place.

First of all it is to be noted that the P_R state may indeed be physiologically relevant [42]. Furthermore, it is highly likely that the E_m^0 of $TyrO^*/TyrO^-$ couple is rather high [4, see also 43], and as a result an electron would rapidly localize on Tyr, and not on heme a_3 , also much faster than the protonation of the BNC. In order to test this, we performed DFT calculations on the P_R state to see if the electron localizes on heme a_3 . Our results suggest that in larger model systems (combining both heme a_3 and Cu_B), the electron preferably reduces the $TyrO^*$, and also irrespective of the protonation state of the proton-loading site (PLS; A-propionate). Furthermore, the distance between the two metals in the BNC is 5-6 Å, and due to the very high rates of electron tunneling at such distances, it is likely that the electron will equilibrate on Tyr due to its much higher operational redox potential [see also ref. 19]. Therefore, in our opinion, the key reason for the non-functional K-channel is the low proton

affinity of TyrO⁻ in the P_R state.

5. Role of K-channel in proton pumping

We have previously speculated that the presence of a positively charged residue (Lys319) in the K-channel of the A-type oxidases may provide an additional advantage of pumping protons at high proton motive force (pmf) [44]. Even though a proton channel exists at the same location in the B- and C-type oxidases, a positively charged residue such as Lys is nevertheless absent. Experimental as well simulation data suggests that protonated Lys undergoes an “UP” flip [37-41,45,46], which brings a positive charge near to the BNC, and increases the redox potential of the latter (by ca. 30 mV). This small increment in the operational E_m of the BNC is probably not critical for the oxidative phase transitions, but may be important for the $\mathbf{O/O_H} \rightarrow \mathbf{E/E_H}$ (and also possibly $\mathbf{E/E_H} \rightarrow \mathbf{R}$) transitions [3]. Without this increment (as in the Lys \rightarrow Met mutation), electron transfer to the BNC is much delayed, and the coupled proton transfer from the N-side to the PLS is also prevented [3,21,22, see also 47]. Therefore, we suggest that the protonated Lys319 and its sidechain dynamics are important in stabilizing the activated $\mathbf{O_H}$ state, in enhancing the rate of the proton-coupled electron transfer (PCET) reaction, and in enabling A-type oxidases to pump protons at high pmf. The absence of D-channel, as well as of the K-channel lysine in the B- and C-type oxidases, render them much more prone to loss of proton pumping at high pmf [48,see also 49]. We have suggested that the substrate protons are not taken up via the K-channel in the oxidative phase of the A-type oxidases due to the acidic properties of Tyr244 (see above). This proposal predicts different acid/base properties of the corresponding active site tyrosine in the B- and C-type oxidases, which can be tested in the future.

Acknowledgements

VS acknowledges postdoctoral funding from the Academy of Finland, and research grants from the Center of Excellence in Biomembrane Research (Academy of Finland). MW acknowledges support from the University of Helsinki, and Societas Scientiarum Fennica, and is grateful to Margareta Blomberg and Per Siegbahn for numerous discussions. We are also thankful to the Center for Scientific Computing (CSC), Finland.

References

1. P. Brzezinski, R. B. Gennis, Cytochrome *c* oxidase: exciting progress and remaining mysteries. *Journal of Bioenergetics and Biomembranes*, 40 (2008) 521-531.
2. S. Yoshikawa, A. Shimada, Reaction mechanism of cytochrome *c* oxidase. *Chemical Reviews*, 115 (2015) 1936-1989.
3. M. Wikström, V. Sharma, V.R. I. Kaila, J. P. Hosler, G. Hummer, New perspectives on proton pumping in cellular respiration. *Chemical Reviews*, 115 (2015) 2196-2221.
4. V. R. I. Kaila, M. I. Verkhovsky, M. Wikström, Proton-coupled electron transfer in cytochrome oxidase. *Chemical Reviews*, 110 (2010) 7062–7081.
5. P. R. Rich, A. Maréchal, Functions of the hydrophilic channels in protonmotive cytochrome *c* oxidase. *Journal of the Royal Society Interface*, 10 (2013) 20130183.
6. M. Wikström, Proton pump coupled to cytochrome *c* oxidase in mitochondria. *Nature*, 266 (1977) 271–273.
7. T. Tsukihara, K. Shimokata, Y. Katayama, H. Shimada, K. Muramoto, H. Aoyama, M. Mochizuki, K. Shinzawa-Itoh, E. Yamashita, M. Yao, Y. Ishimura, S. Yoshikawa, The low-spin heme of cytochrome *c* oxidase as the driving element of the proton-pumping process. *Proceedings of the National Academy of Sciences of the United States of America*, 100 (2003) 15304-15309.
8. T. Tsukihara, H. Aoyama, E. Yamashita, T. Tomizaki, H. Yamaguchi, K. Shinzawa-Itoh, R. Nakashima, R. Yaono, S. Yoshikawa, The whole structure of the 13-subunit oxidized cytochrome *c* oxidase at 2.8 Å. *Science*, 272 (1996) 1136-1144..
9. S. Iwata, C. Ostermeier, B. Ludwig, H. Michel, Structure at 2.8 Å resolution of cytochrome *c* oxidase from *Paracoccus denitrificans*. *Nature*, 376 (1995) 660-669.
10. J. Abramson, S. Riistama, G. Larsson, A. Jasaitis, M. Svensson-Ek, L. Laakkonen, A. Puustinen, S. Iwata, M. Wikström, The structure of the ubiquinol oxidase from *Escherichia coli* and its ubiquinone binding site. *Nature Structural & Molecular Biology*, 7 (2000) 910-917.
11. T. Tiefenbrunn, W. Liu, Y. Chen, V. Katritch, C.D. Stout, J.A. Fee, V. Cherezov, High Resolution Structure of the *ba*₃ Cytochrome *c* Oxidase from *Thermus thermophilus* in a Lipidic Environment. *PLoS One*, 6 (2011) e22348.

12. M. Wikström, Energy-dependent reversal of the cytochrome oxidase reaction. *Proceedings of the National Academy of Sciences of the United States of America*, 78 (1981) 4051-4054.
13. L. Weng, G. M. Baker, Reaction of hydrogen peroxide with the rapid form of resting cytochrome oxidase. *Biochemistry*, 30 (1991) 5727-5733.
14. B. Chance, C. Saronio, J. S. Leigh, Functional intermediates in the reaction of membrane-bound cytochrome oxidase with oxygen. *Journal of Biological Chemistry*, 250 (1975) 9226-9237.
15. S. W. Han, Y. C. Ching, D. L. Rousseau, Primary intermediate in the reaction of oxygen with fully reduced cytochrome *c* oxidase. *Proceedings of the National Academy of Sciences of the United States of America*, 87 (1990) 2491-2495.
16. S. A. Siletsky, A. A. Konstantinov, Cytochrome *c* oxidase: Charge translocation coupled to single-electron partial steps of the catalytic cycle. *Biochimica et Biophysica Acta (BBA) - Bioenergetics*, 1817 (2012) 476-488.
17. I. Belevich, M. Verkhovsky, Molecular mechanism of proton translocation by cytochrome *c* oxidase. *Antioxidants and Redox Signaling*, 10 (2008) 1-29.
18. M. M. Pereira, M. Santana, M. Teixeira, A novel scenario for the evolution of haem-copper oxygen reductases. *Biochimica et Biophysica Acta (BBA) - Bioenergetics*, 1505 (2001) 185-208.
19. V. Sharma, K. D. Karlin, M. Wikström, Computational study of the activated O_H state in the catalytic mechanism of cytochrome *c* oxidase. *Proceedings of the National Academy of Sciences of the United States of America*, 110 (2013) 16844-16849.
20. M. R. A. Blomberg, Mechanism of oxygen reduction in cytochrome *c* oxidase and the role of the active site tyrosine. *Biochemistry*, 55 (2016) 489-500.
21. D. Bloch, I. Belevich, A. Jasaitis, C. Ribacka, A. Puustinen, M. I. Verkhovsky, M. Wikström, The catalytic cycle of cytochrome *c* oxidase is not the sum of its two halves. *Proceedings of the National Academy of Sciences of the United States of America*, 101 (2004) 529-533.

22. I. Belevich, D. A. Bloch, N. Belevich, M. Wikström, M. I. Verkhovsky, Exploring the proton pump mechanism of cytochrome *c* oxidase in real time. *Proceedings of the National Academy of Sciences of the United States of America*, 104 (2007) 2685–2690.
23. A.A. Konstantinov, S. Siletsky, D. Mitchell, A. Kaulen, R. B. Gennis, The roles of the two proton input channels in cytochrome *c* oxidase from *Rhodobacter sphaeroides* probed by the effects of site-directed mutations on time-resolved electrogenic intraprotein proton transfer, *Proceedings of the National Academy of Sciences of the United States of America*, 94 (1997) 9085-9090.
24. E. A. Gorbikova, I. Belevich, M. Wikström, M. I. Verkhovsky, The proton donor for O-O bond scission by cytochrome *c* oxidase. *Proceedings of the National Academy of Sciences of United States of America*, 105 (2008) 10733-10737.
25. E. A. Gorbikova, M. Wikström, M. I. Verkhovsky, The protonation state of the cross-linked tyrosine during the catalytic cycle of cytochrome *c* oxidase. *Journal of Biological Chemistry*, 283 (2008) 34907–34912.
26. M. Wikström, M. I. Verkhovsky, G. Hummer, Water-gated mechanism of proton translocation by cytochrome *c* oxidase. *Biochimica et Biophysica Acta (BBA) - Bioenergetics*, 1604 (2003) 61–65.
27. V. Sharma, G. Enkavi, I. Vattulainen, T. Rog, M. Wikström, Proton-coupled electron transfer and the role of water molecules in proton pumping by cytochrome *c* oxidase. *Proceedings of the National Academy of Sciences of United States of America*, 112 (2015) 2040-2045.
28. A. Tuukkanen, M.I. Verkhovsky, L. Laakkonen, M. Wikström, The K-pathway revisited: A computational study on cytochrome *c* oxidase. *Biochimica et Biophysica Acta (BBA) – Bioenergetics* 1757 (2006) 1117-1121.
29. P. E. M. Siegbahn, M. R. A. Blomberg, M. L. Blomberg, Theoretical study of the energetics of proton pumping and oxygen reduction in cytochrome oxidase. *Journal of Physical Chemistry B* 107 (2003) 10946-10955.
30. Y. Song, E. Michonova-Alexova, M. R. Gunner, Calculate proton uptake on anaerobic

- reduction of cytochrome *c* oxidase: Is the reaction electroneutral? *Biochemistry* 45 (2006) 7959-7975.
31. N. Ghosh, X. Prat-Resina, M. R. Gunner, Q. Cui, Microscopic pKa analysis of Glu286 in cytochrome *c* oxidase (*Rhodobacter sphaeroides*): Towards a calibrated molecular model. *Biochemistry* 48 (2009) 2468-2485.
32. V. R. I. Kaila, M. P. Johansson, D. Sundholm, L. Laakkonen, M. Wikström, The chemistry of the Cu_B site in cytochrome *c* oxidase and the importance of its unique His-Tyr bond. *Biochimica et Biophysica Acta (BBA) - Bioenergetics*, 1787 (2008) 221-233.
33. G. Bränden, R. B. Gennis, P. Brzezinski, Transmembrane proton translocation by cytochrome *c* oxidase. *Biochimica et Biophysica Acta (BBA) - Bioenergetics*, 1757 (2006) 1052-1063.
34. M. R. A. Blomberg, P. E. M. Siegbahn, How cytochrome *c* oxidase can pump four protons per oxygen molecule at high electrochemical gradient. *Biochimica et Biophysica Acta (BBA) - Bioenergetics*, 1847 (2015) 364-375.
35. M. R. A. Blomberg, P. E. M. Siegbahn, Protonation of the binuclear active site in cytochrome *c* oxidase decreases the reduction potential of Cu_B. *Biochimica et Biophysica Acta (BBA) - Bioenergetics*, 1847 (2015) 1173-1180.
36. L. Qin, J. Liu, D. A. Mills, D. A. Proshlyakov, C. Hiser, S. Ferguson-Miller, Redox-dependent conformational changes in cytochrome *c* oxidase suggest a gating mechanism for proton uptake. *Biochemistry*, 48 (2009) 5121-5130.
37. J. A. Lyons, D. Aragão, O. Slattery, A. V. Pislakov, T. Soulimane, M. Caffrey, Structural insights into electron transfer in *caa*₃-type cytochrome oxidase. *Nature* 487 (2012) 514-520.
38. I. Hofacker, K. Schulten, Oxygen and proton pathways in cytochrome *c* oxidase. *Proteins* 30 (1998) 100-107.
39. E. Olkhova, M. C. Hutter, M. A. Lill, V. Helms, H. Michel, Dynamic water networks

- in cytochrome *c* oxidase from *Paracoccus denitrificans* investigated by molecular dynamics simulations. *Biophysical Journal*, 86 (2004) 1873-1889.
40. J. Koepke, E. Olkhova, H. Angerer, H. Müller, G. Peng, H. Michel, High resolution crystal structure of *Paracoccus denitrificans* cytochrome *c* oxidase: New insights into the active site and the proton transfer pathways. *Biochimica et Biophysica Acta (BBA) - Bioenergetics*, 1787 (2009) 635-645.
 41. A. L. Woelke, G. Galstyan, E. W. Knapp, Lys 362 in cytochrome *c* oxidase regulates opening of the K-channel via changes in pKa and conformation. *Biochimica et Biophysica Acta (BBA) - Bioenergetics*, 1837 (2014) 1998-2003.
 42. M. Wikström, Active site intermediates in the reduction of O₂ by cytochrome oxidase, and their derivatives, *Biochimica et Biophysica Acta (BBA) - Bioenergetics*, 1817 (2012) 232-240.
 43. C. Tommos, G. T. Babcock, Proton and hydrogen currents in photosynthetic water oxidation. *Biochimica et Biophysica Acta (BBA) - Bioenergetics*, 1458 (2000) 199-219.
 44. V. Sharma, M. Wikström, A structural and functional perspective on the evolution of the heme-copper oxidases. *FEBS Letters*, 588 (21) 3787-3792.
 45. M. Branden, H. Sigurdson, A. Namslauer, R. B. Gennis, P. Adeloeth, P. Brzezinski, On the role of the K-proton transfer pathway in cytochrome *c* oxidase. *Proceedings of the National Academy of Sciences of the United States of America*, 98 (2001) 5013-5018.
 46. M. Rintanen, I. Belevich, M. I. Verkhovsky, Electrogenic events upon photolysis of CO from fully reduced cytochrome *c* oxidase. *Biochimica et Biophysica Acta (BBA) – Bioenergetics* 1817 (2012) 269-275.
 47. A. Jünemann, B. Meunier, R. B. Gennis, P. R. Rich, Effects of mutation of the conserved Lysine-362 in cytochrome *c* oxidase from *Rhodobacter sphaeroides*. *Biochemistry* 36 (1997) 14456-14464.
 48. V. Rauhamäki, M. Wikström, The causes of reduced proton-pumping efficiency in type B and C respiratory heme-copper oxidases, and in some mutated variants of type A. *Biochimica et Biophysica Acta (BBA) - Bioenergetics* 1837 (2014) 999-1003.
 49. C. von Ballmoos, P. Adeloeth, R. B. Gennis, P. Brzezinski, Proton transfer in *ba*₃ cytochrome *c* oxidase from *Thermus thermophilus*. *Biochimica et Biophysica Acta*

(BBA) - Bioenergetics 1817 (2012) 650-657.

Figure legends

Fig. 1. Basic structure of cytochrome *c* oxidase from *Bos taurus* (PDB id : 1V54) [7]. Electron transfer from Cu_A, via heme *a*, to the active site of oxygen reduction (BNC) is shown by a black arrow. Protons are transferred to the active site through two proton pathways (D- and K- channels, orange arrows), which are named based on conserved amino acid residues D91 and K319, respectively. The catalytically active tyrosine (Y244, green) is covalently linked to the histidine ligand (H240, blue) of Cu_B (orange). Purple spheres are water molecules observed in the crystal structure.

Fig. 2. Catalytic intermediates of CcO in the “oxidative phase” where the reduced enzyme reacts with O₂. Initial steps of oxygen binding and reduction (**R** → **A** → **P_M**), and charge translocation events (**P_R** → **F** → **O**) are shown. The redox states of heme *a*₃ (Fe), Cu_B and the cross-linked tyrosine (Tyr244), as well as the protonation states of the oxygenous ligand of the metals and Tyr244 are displayed. TyrO* depicts the neutral free radical form of the tyrosine. The Cu_B-bound hydroxide ligand is displayed as HO⁻ or OH⁻.

Fig. 3 Water arrays from the D-channel end-point E242 (A), and from the K-channel lysine (K319) (B) to the binuclear center, as observed in molecular simulations of the **P_R** state. In A, E242 adopts an “UP” conformation stabilising a water wire into the BNC via Cu_B. In B, protonated K319 adopts “UP” conformation, stabilizing a water wire towards the active site via tyrosine (Y244).

Figure 1
[Click here to download high resolution image](#)

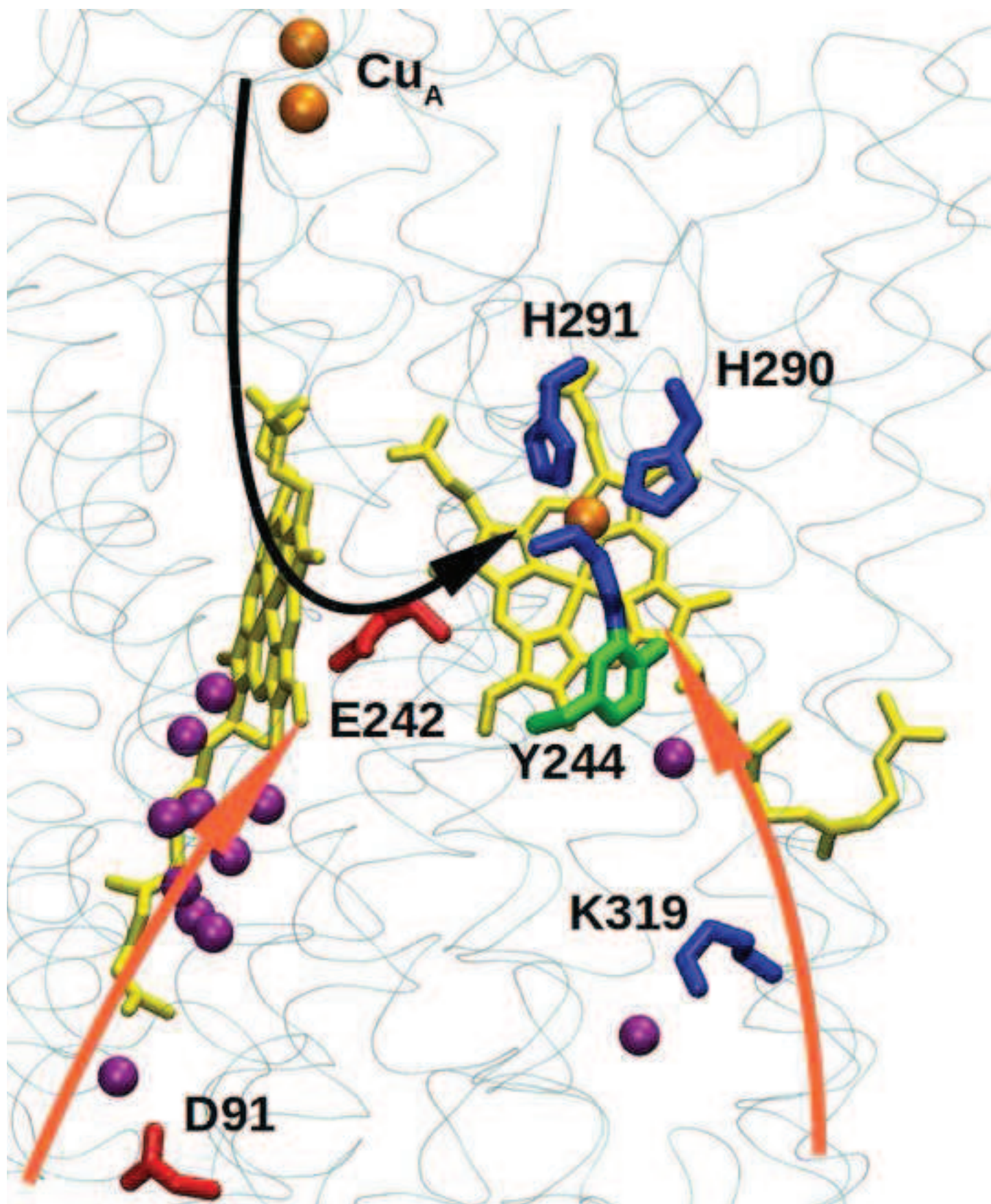


Figure 2
[Click here to download high resolution image](#)

